Tree Physiology 25, 1161–1172

Expression of senescence-associated genes in the leaves of silver birch (*Betula pendula*)

MAARIT SILLANPÄÄ,[1–3] SARI KONTUNEN-SOPPELA,[2] EEVA-MARIA LUOMALA,[4] SIRKKA SUTINEN,[4,5] JAAKKO KANGASJÄRVI,[1,6] HELY HÄGGMAN[2,7] and ELINA VAPAAVUORI[4,8]

[1] *Institute of Biotechnology, The Viikki Biocenter, University of Helsinki, P.O. Box 56, FIN-00014 Helsinki, Finland*

[2] *Finnish Forest Research Institute, Punkaharju Research Station, FIN-58450 Punkaharju, Finland*

[3] *Current address: National Public Health Institute, Mannerheimintie 166, 00300 Helsinki, Finland*

[4] *Finnish Forest Research Institute, Suonenjoki Research Station, FIN-77600 Suonenjoki, Finland*

[5] *Current address: Finnish Forest Research Institute, Joensuu Research Centre, PL 68, 80101 Joensuu, Finland*

[6] *Current address: Department of Biosciences, Plant Physiology, University of Helsinki, FIN-00014 Helsinki, Finland*

[7] *Department of Biology, University of Oulu, P.O. Box 3000, FIN-90014 Oulu, Finland*

[8] *Corresponding author (elina.vapaavuori@metla.fi)*

Received April 19, 2004; accepted January 15, 2005; published online July 4, 2005

Summary Development was monitored throughout the entire life span of silver birch (*Betula pendula* Roth.) leaves. The focus was on senescence-related changes in photosynthesis and gene expression. The youngest fully developed leaves were compared with older senescing leaves in two silver birch lines: the wild-type line R and a late-senescing line R3.1. Line R3.1 was found among transgenic lines produced with a plasmid containing sense-*RbcS* and *nptII* under the control of the 35S CaMV promoter. Compared with the wild type, line R3.1 showed no general change in the mRNA levels of *RbcS* or Rubisco protein; therefore, it can be considered a line whose phenotype is due to insertional mutagenesis. Leaf senescence started earlier in line R than in line R3.1. Senescence was characterized by declining photosynthesis as indicated by decreases in chlorophyll fluorescence, the amount and activity of Rubisco, and the level of the ribulose-1,5-bisphosphate carboxylase/oxygenase small subunit (*RbcS1*) mRNA. Some well-known senescence-associated genes (SAGs) encoding cysteine proteinases (*Cyp1*, *Cyp2*) and a pathogenesis-related gene (*Pr1*) were associated with leaf senescence. The expression pattern of *Cyp1* indicated that it could serve as a molecular marker of leaf senescence in silver birch. Several genes related to energy metabolism, antioxidants and phenylpropanoid biosynthesis showed enhanced expression during leaf senescence. A distinct pattern in transcript abundance during leaf development was revealed for some of the identified SAGs.

Keywords: antioxidants, cysteine proteinases, energy metabolism, pathogenesis-related genes, late senescing mutant, phenylpropanoid biosynthesis, photosynthesis, Rubisco.

Introduction

Senescence is the highly organized, final stage of leaf development during which leaf nutrients are mobilized and recycled. During senescence many functional and structural changes occur at the organelle level (Smart 1994, Gepstein 2004). At first, changes occur in chloroplasts while photosynthetic rate declines (Gepstein 1988), but mitochondria and the nucleus remain intact until an advanced stage of senescence (Smart 1994, Inada et al. 1998). Catabolism of membrane lipids, proteins and nucleic acids requires synthesis of new proteins and enhanced transcription of the corresponding genes. Recently, a number of senescence-associated genes (SAGs) have been identified (Gan and Amasino 1997, Gepstein et al. 2003, Gepstein 2004). Some SAGs encode proteins needed for catabolism, such as proteases, lipases and ribonucleases (Buchanan-Wollaston 1997).

The regulation of leaf senescence involves both environmental factors, for example light quality and photoperiod (Smart 1994), and internal metabolic signals, such as sugars and nitrogen (Masclaux et al. 2000), production of reactive oxygen species (ROS) (Thompson et al. 1987) and the plant hormones ethylene and cytokinin (Smart 1994). Leaf age can also be a signal for senescence (Hensel et al. 1993). There is evidence that crosstalk between many signalling pathways affects leaf senescence, and some signals might activate several pathways (Bowler and Fluhr 2000, Buchanan-Wollaston et al. 2003).

Delayed leaf senescence has been observed in transgenic P_{SAG12}-*IPT* tobacco (*Nicotiana tabacum* L.) plants that produce cytokinins in senescing leaves (Jordi et al. 2000), in tobacco plants overexpressing a homeobox gene *knotted1* (Ori et

al. 1999), and in ribulose-1,5-bisphosphate carboxylase/oxygenase (Rubisco) antisense tobacco (Miller et al. 2000). Several stay-green mutants have been characterized in cereals, grasses, legumes and trees (Thomas and Smart 1993). For example, *Festuca pratensis* Huds. was found to have a non-functional enzyme of the chlorophyll degradation pathway (Vicentini et al. 1995), and in soybean (*Glycine max* (L.) Merrill) chloroplasts, membrane degradation was prevented in an unknown way (Guiamét and Giannibelli 1994). Although it is not known how these individual changes interact with other senescence-controlling signals to delay leaf senescence, it is evident that the onset and progression of leaf senescence involves several genes.

Natural leaf senescence in woody species has rarely been studied (Vapaavuori and Vuorinen 1989, Brendley and Pell 1998, Pell et al. 1999) and only in the context of declining photosynthetic activity. Recently, the gene expression pattern in naturally senescing aspen (*Populus tremula* L.) leaves was examined by the microarray technique (Bhalerao et al. 2003, Andersson et al. 2004) and many SAGs previously reported in annual plants were found to function during aspen leaf senescence. In previous studies with young silver birch (*Betula pendula* Roth) seedlings (Valjakka et al. 1999), we showed that, along with senescence-related physiological phenomena, the transcript levels of leucine aminopeptidase (*Lap*) and pathogenesis-related protein 10 (*Ypr10*) become more abundant in senescing leaves.

To further elucidate the regulation of leaf senescence in silver birch, we investigated the roles of developmental stage and leaf age in determining the onset of senescence in two silver birch lines growing under controlled conditions in a greenhouse. In addition to a wild type line R, a sense ribulose-1,5-bisphosphate carboxylase/oxygenase small subunit (*RbcS*) line R3.1 of the same clone, containing the birch endogenous Rubisco small subunit under a constitutive promoter, was studied. The transgenic line R3.1 shows delayed senescence (Valjakka et al. 2000). To monitor leaf development and senescence during plant growth and growth cessation, senescing leaves situated on the lower stem were compared with the youngest fully developed leaves on the upper stem of these birch lines. The onset and development of senescence were studied at the physiological, biochemical and molecular levels.

Materials and methods

Plant material, growth and experimental design

We studied transgenic sense-*RbcS* line R3.1 and wild-type line R silver birch plants of clone R, which is a progeny of two selected trees originating from southern Finland. Line R3.1, which shows delayed senescence, was found among the transgenic lines produced with the sense-*RbcS* construct (Valjakka et al. 2000). In line R3.1, a fragment of silver birch *RbcS1* cDNA, containing the mature Rubisco small subunit, is inserted in sense orientation under the control of the 35S CaMV promoter. This line has five to six copies of the transferred gene (Valjakka et al. 2000). In vitro plantlets were replicated before they were transferred to a mixture of unfertilized and Ca-free peat (Kekkilä, Finland), perlite and forest soil (2:2:1, v/v) at high humidity for 2 weeks. On Day 0 of this experiment, they were planted in 0.7-l pots containing fertilized peat (Kekkilä, Finland). The experiment was carried out in a greenhouse during September and October. A 16-h photoperiod was maintained with high-pressure sodium vapor discharge lamps (SON-T AGRO-400 W, Philips), which supplied additional photosynthetically active radiation (PAR) of 300 μmol m^{-2} s^{-1} at the shoot-tip level. Mean day/night air temperature was 21/20 °C, and relative humidity was > 40%.

One hundred plants of each line were arranged in four blocks according to height from the shortest to the tallest. Each block consisted of 25 plants of both lines R and R3.1 in random order. To create similar light conditions for all plants, each block was surrounded by an extra row of silver birch plants. At the beginning of the experiment, five plants in each block were randomly selected for repeated measurements of growth and chlorophyll fluorescence, and were used in the final sampling, and then harvested for biomass determination. Samples were collected 23, 34, 44, 56 and 69–70 days after the beginning of the experiment. Leaf senescence was followed in leaves that were marked as the life span leaves 1 day before the first sampling. On Day 0, the life span leaves were at the third and fourth node from the apex (Figure 1B). Leaves selected for measurements were the youngest fully developed (yfd) leaves on the plants. As the line R plants grew during the study, the position of the life span leaves changed relative to the yfd leaf (Figure 1B). Because line R3.1 plants only produced 4–7 small leaves during the study (Figure 1B), there were no yfd leaves on the first three measurement dates, and for the last two sampling days when the plants had yfd leaves, the life span leaves of this line also represented the youngest fully developed leaves.

All samples were taken between 1300 and 1600 h, and at each sampling time, five plants per line were randomly selected from each replicate block. The lengths and widths of the pre-selected leaves were measured. The leaves were then excised and frozen in liquid nitrogen. Leaf area was calculated from the correlation between the measured leaf area (LI-3050A, Li-Cor, Lincoln, NE) and leaf length × leaf width. For biochemical analyses, the leaves from each replicate block were pooled. After each sampling, the stem, roots and remaining leaves were harvested for fresh and dry mass determinations (60 °C for 48 h).

Chlorophyll fluorescence

Chlorophyll fluorescence of the life span leaves and yfd leaves was measured at the growth temperature with a portable, pulse-amplitude-modulated fluorometer (MINI-PAM, Heinz Walz GmbH, Effeltrich, Germany). After 15 min of dark adaptation in a dark leaf clip (DLC-8, Heinz Walz GmbH), the minimal fluorescence (F_0) with all PSII reaction centers open was determined with a low-intensity modulated measuring light (< 0.1 μmol m^{-2} s^{-1}). A 1.0-s white light pulse of about 9000 μmol m^{-2} s^{-1} produced transient closure of PSII reaction

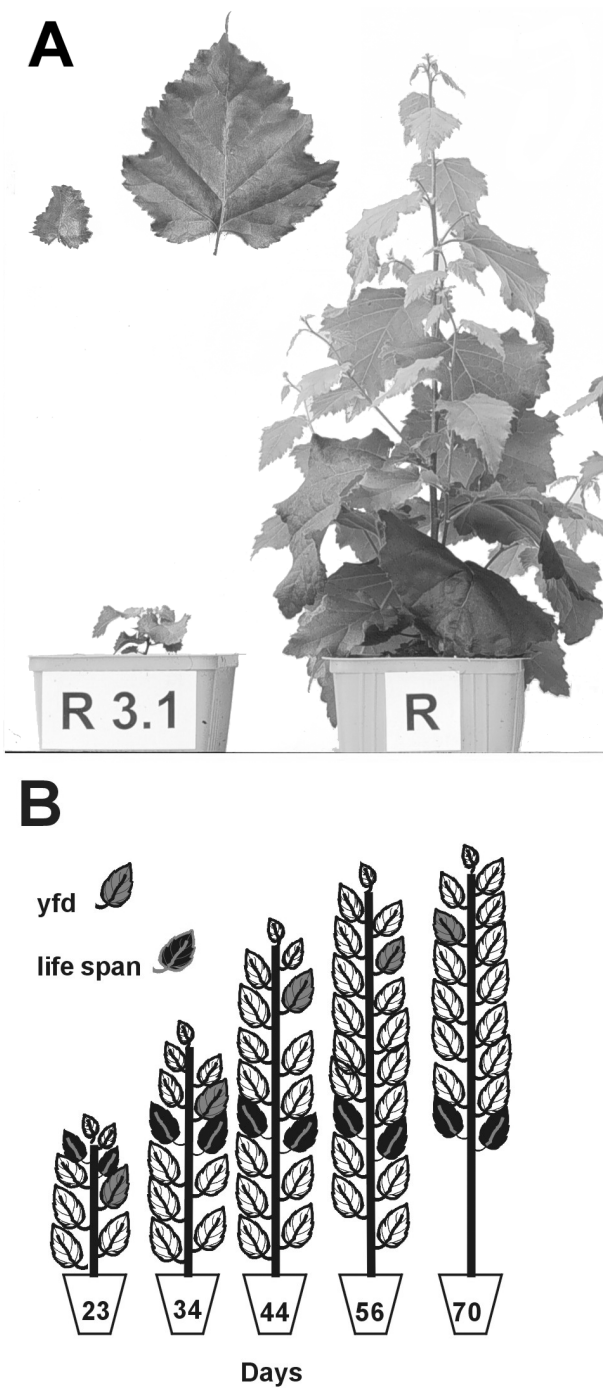

Figure 1. (A) Plants from silver birch lines R and R3.1 and the youngest fully expanded leaves on Day 28. (B) Position of the life span leaves and the youngest fully developed (yfd) leaves of line R plants on the days when the measurements were made during the experiment (Days 23, 34, 44, 57 and 69–70).

centers, and maximal fluorescence (F_m) was recorded. During all measurements, the measuring pulse frequency was set at 0.6 kHz. The maximal quantum yield of PSII photochemistry in the dark-adapted state (F_v/F_m) was calculated as ($F_m - F_0$)/F_m (Genty et al. 1989). After the saturating pulse, the leaves were exposed to actinic light of 360– 475 µmol m^{-2} s^{-1} (Figure 3B) for 2 min, after which steady-state fluorescence (F_s) was recorded, and a saturating pulse was applied to determine the maximal fluorescence at steady-state (F_m'). The apparent quantum yield of PSII photochemistry in the light-adapted steady state (F_v'/F_m') was calculated as ($F_m' - F_s$)/F_m' (Genty et al. 1989) and non-photochemical quenching (NPQ) as ($F_m - F_m'$)/F_m', according to the Stern-Volmer equation (Bilger and Björkman 1990).

Gas exchange

Gas exchange was measured with an open, portable photosynthesis system (LI-6400, Li-Cor) with a standard leaf chamber equipped with a 6400-02B LED light source (LI-6400, Li-Cor). Gas exchange parameters were calculated according to the method of von Caemmerer and Farquhar (1981). Measurements were made in the greenhouse under the experimental growth conditions. During measurements, leaf temperature was maintained at 22 °C with a Peltier element.

On Day 49, we measured gas exchange of the yfd leaf from 20 plants of line R and six plants of line R3.1. The CO_2 concentration ([CO_2]) in the leaf chamber was 360 ppm, relative humidity (RH) was 40%, and photon flux density was saturating (PAR = 800 µmol m^{-2} s^{-1}). On Days 48 and 51, apparent quantum yield (i.e., the initial slope of the light response curve, α) was determined in four plants per line. The [CO_2] in the leaf chamber was 360 ppm, and RH was adjusted to 40–55%. Net photosynthesis (P_n) was first allowed to stabilize at 500 µmol m^{-2} s^{-1} (PAR), after which P_n was recorded as PAR was decreased to < 180 µmol m^{-2} s^{-1} in three or four steps. On Days 50 and 51, the maximum velocity of the Rubisco carboxylation of RuBP (i.e., the carboxylation efficiency, V_{max}) was measured on six (line R) or five (line R3.1) plants. The RH was 40–60%, and PAR was saturating for P_n. After the leaf was inserted in the chamber, P_n was allowed to stabilize at 360 ppm [CO_2], after which it was measured as the [CO_2] was increased from 40 to 170 ppm in four steps. The values obtained were then corrected for chamber leaks. During measurements of α and V_{max}, P_n was allowed to stabilize for 1 to 3 min at each step, so that CV was < 1%.

Activity and amount of Rubisco and amounts of soluble protein and chlorophyll

Leaves were ground to a fine powder in liquid nitrogen, and a sample of about 30 mg was homogenized in ice-cold extraction buffer containing 50 mM MES, pH 6.8, 20 mM $MgCl_2$, 50 mM 2-mercaptoethanol and 1% (v/v) Tween 80. Aliquots of the crude extract were analyzed for chlorophyll content by the method of Porra (1989). After centrifugation, the total activity of Rubisco (EC 4.1.1.39) was determined as the incorporation of ^{14}C into acid-stable products (Laitinen et al. 2000). The amount of Rubisco protein was determined by polyacrylamide gel electrophoresis (Ruuska et al. 1994) and the soluble protein content was determined by Bradford's method (Bradford 1976).

Electron microscopy

Three plants of each line and replicate were selected at random for ultrastructural studies. At the last sampling, Days 69–70, the yfd leaf from each replicate was removed and fixed in a mixture of 1.5% glutaraldehyde, 1.5% paraformaldehyde and 0.05 M cacodylate buffer (pH 7.0, containing 0.15 M sucrose and 2 mM $CaCl_2$). Cross sections were taken from the middle of the leaves near the central vein and fixed at 4 °C for about 22 h. Further stages of fixation were carried out as described by Soikkeli (1980). For electron microscopy, one plant per line and replicate was randomly selected for cross-sectioning of the leaves. The sections were then stained with uranyl acetate and lead citrate. The palisade and spongy cells were photographed at a magnification of 7500× with a transmission electron microscope (JEOL JEM-1200 EX) equipped with a digital camera. The mean areas of chloroplasts, starch grains and mitochondria were measured by the point-counting method (Romppanen and Collan 1984) using the Adobe Photoshop 4.0.1 program.

Analysis of gene expression

Total RNA was isolated according to Chang (1993) from pooled leaf samples that represented all four replicates. Because of the small sample size in line R3.1, gene expression could be analyzed only on the last 3 days of sampling. The quality of the RNA samples was verified by Northern hybridizations (Sambrook et al. 1989). For analysis of RNA dot blot hybridization, equal amounts of total RNA (3 µg) were diluted as described by Valjakka et al. (1999). Samples were blotted with a Minifold vacuum filtration system (Schleicher and Schuell, Dassel, Germany) onto a positively charged nylon membrane (Boehringer Mannheim, Mannheim, Germany).

The PCR-amplified fragments of silver birch cDNAs were prepared at the Helsinki Institute of Biotechnology, University of Helsinki, by the research groups of Prof. E.T. Palva and Prof. J. Kangasjärvi. These fragments, which represented genes encoding enzymes of different metabolic functions (Table 3), were purified with QIAquick PCR Purification Kit (Qiagen, Hilden, Germany) and then labeled for analysis of northern and RNA-dot blot hybridization with Ready-to-go DNA labeling beads (–dCTP) (Amersham Pharmacia Biotech) in a volume of 50 µl with [$-^{32}$Pα]dCTP (10 mCi ml^{-1}). Labeled probes were purified on G-50 columns (ProbeQuant G-50 Micro Columns, Amersham Pharmacia Biotech). Northern and RNA dot blot hybridizations were performed in a modified Church buffer: 0.5 M $NaHPO_4$, 7% SDS at 65 °C (Church and Gilbert 1984). Post-hybridization washes were performed with 5% SEN (5% SDS, 1 mM EDTA, pH 8, 40 mM $NaHPO_4$) and 1% SEN (1% SDS, 1 mM EDTA, pH 8, 40 mM $NaHPO_4$) solutions at 65 °C; and the membranes were rinsed in 2× SSC (3 M NaCl + 0.3 M sodium citrate) before being exposed to phosphor imager screens (BAS-1500, Fuji film, Kanagawa, Japan). The signal intensity was quantified using Tina 2.09 software (Raytest, Isotopenmessgeräte GmbH, Germany). Probes were removed from the membranes before they were re-hybridized with a ribosomal 18S probe.

For reverse Northern hybridization, PCR products (100 ng) were suspended in 0.2 N NaOH and blotted with a Minifold vacuum filtration system onto nylon membranes. The controls included *Arabidopsis* actin 2 (Genbank AC H36835, 179M16T7) as a constitutive control and poly(T) 21-mer, bluescript, pGEM3Z, pSPORT and pUC19 as negative controls. The DNase-treated total RNA was used for poly(A)$^+$ RNA purification (Oligotex mRNA midi kit, Qiagen GmbH, Hilden, Germany). The mRNA samples were reverse-transcribed in the presence of [α-^{33}P] dCTP 10 mCi ml^{-1} (Amersham). The reverse transcription reaction was performed in 25 µl of solution containing 1 µg poly(A) RNA with 660 ng oligo(dT) 21-mer, 500 ng oligo(dT) 15-mer, 520 µM each of dATP, dGTP and dTTP, 5 µM dCTP, 5 µl [α-^{33}P] dCTP (10 µCi µl^{-1}), 200 U M-MVL reverse transcriptase (Promega, Madison, WI) in 1 × M-MVL buffer. After a 1-h incubation at 42 °C, the reaction was denatured at 70 °C for 15 min, 2 U of RNaseH was added and the reaction mixture was incubated at 37 °C for 30 min. The probes were purified on G-50 columns.

Reverse Northern membranes were prehybridized for 1–2 h in a solution containing 50% formamide, 1 × Denhart's solution (1% (v/v) Ficoll 400, 1% (w/v) polyvinylpyrrolidone, 1% (w/v) bovine serum albumin), 5 × SSC, 1% (w/v) SDS, and 0.25 mg ml^{-1} herring sperm DNA. The membranes were hybridized overnight. After hybridization, high stringency washes were performed at 65 °C. Filters were exposed to phosphor imager screens and the signal intensity was quantified using Tina 2.09 software. Alterations in gene expression were normalized based on the abundance of actin 2, which was used as a constitutive control. In some of the leaf samples, the magnitude of the change in gene expression was difficult to assess, because the initial expression level of some genes in the yfd leaves was low: these genes are given the notation "weak signal (ws)" in Table 3.

Statistical analyses

Net photosynthesis and electron microscopy results were analyzed with *t* tests (SPSS 8.0).

Results

Growth characteristics

Phenotypic differences between the transgenic line R3.1 and the wild type R line plants were large. Height growth was low in line R3.1 (Figure 2A), the internodes were short and the fully developed leaves were small and curly in comparison with those of line R (Figures 1A and 2C). Leaf area growth of life span leaves was severely reduced in line R3.1 compared with R (Figure 2C). The life span leaves of line R attained maximal area on Day 34 when the life span leaves of line R3.1 were still expanding (Figure 2C). Height growth of line R plants stopped 44 days after the start of the experiment (Figure 2A) and terminal buds formed. After Day 44, yfd leaves of line R did not grow as large as yfd leaves that developed during the period of height growth (Figures 2A and 2C). The total biomass of line R3.1 plants was always less than that of line R

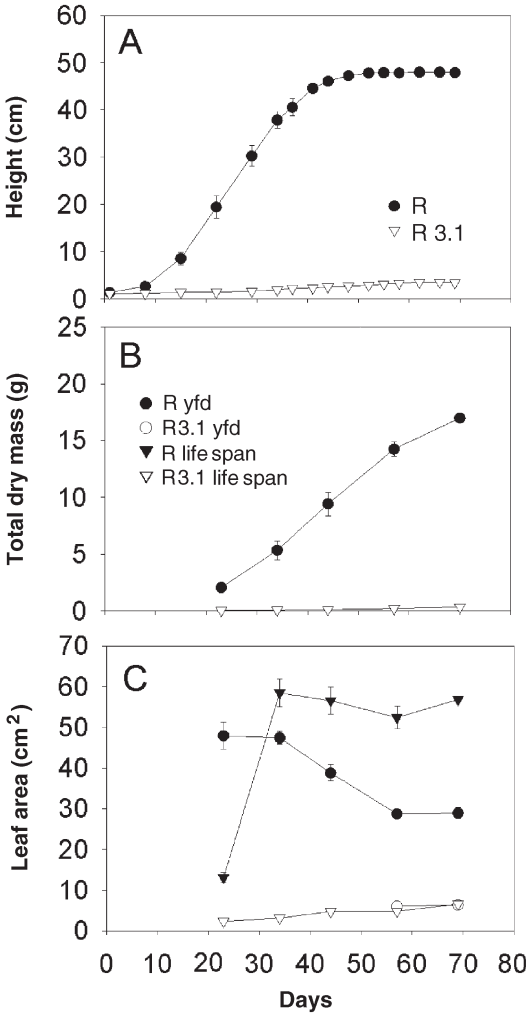

Figure 2. Height growth (A), total biomass (leaves, stem and roots) production (B) and development of leaf area in life span leaves and in the youngest fully developed (yfd) leaves (C) of silver birch lines R and R3.1. All measurements were made on Days 23, 34, 44, 57 and 69–70. Mean ± SE, n = 20 in (A) and (B), n = 1–20 in (C).

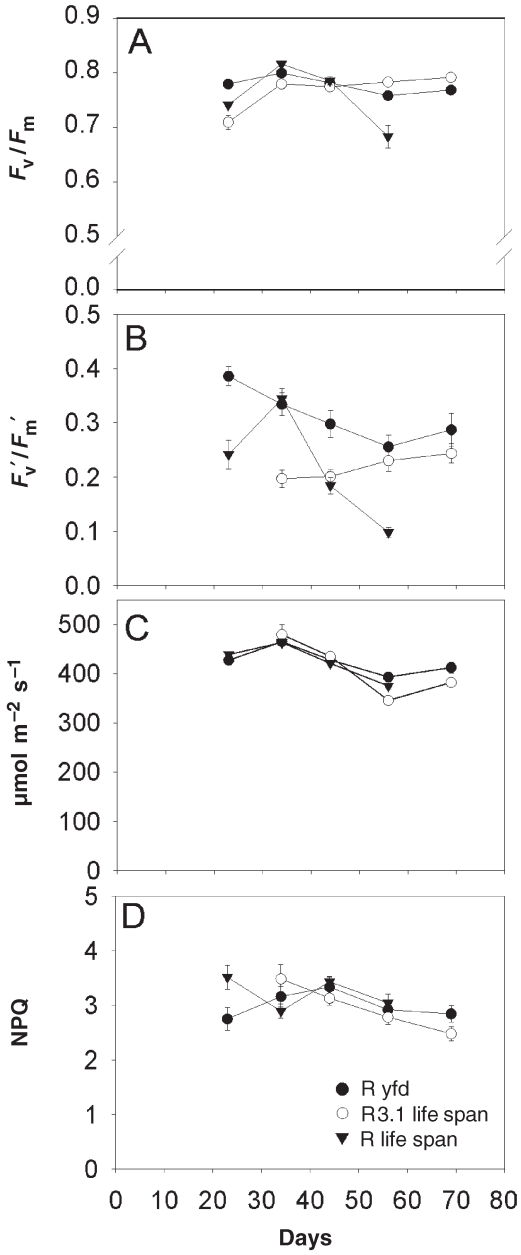

Figure 3. (A) Maximal efficiency of photosystem II (F_v/F_m) measured as chlorophyll fluorescence in the dark-adapted state in the youngest fully developed leaves of line R and in life span leaves of silver birch lines R3.1 and R. (B) Actual efficiency of photosystem II (F_v'/F_m') measured as chlorophyll fluorescence in the light in the same leaves as in A. (C) Irradiances during the measurements. (D) Non-photochemical quenching (NPQ) measured in the same leaves as in A. All measurements were made on life span leaves on Days 23, 34, 44 and 57 and on the youngest fully developed (yfd) leaves on Days 23, 34, 44, 57 and 69–70. Mean ± SE, n = 6–20.

plants (Figure 2B), but despite the cessation of height growth, it continued to increase in both lines until the end of the study. Leaves of line R3.1 remained green throughout the experiment, whereas the lowest leaves of line R became yellow and abscised.

Characteristics of photosynthesis

Maximum photochemical efficiency of PSII, measured as chlorophyll fluorescence of dark-adapted leaves (F_v/F_m) as well as apparent quantum yield of PSII (F_v'/F_m') decreased from Day 34 (Figure 3A) in the life span leaves of line R. The life span leaves of line R3.1 showed similar F_v/F_m to the yfd leaves of line R, both remaining high throughout the experiment (Figure 3A). Apparent quantum yield decreased from 0.4 to 0.3 in yfd leaves of line R, whereas in line R3.1, it remained stable (Figure 3B). There were no changes in non-photochemical quenching (NPQ) during the experiment or between the lines (Figure 3D).

On Day 49, there were no significant differences between lines in net photosynthesis, stomatal conductance or intercellular CO_2 concentration (Table 1). Leaf area of yfd leaves was several times larger in line R plants than in line R3.1 plants, indicating much greater net carbon gain in line R leaves

compared with line R3.1 leaves (Figure 2C). Apparent quantum yield measured on Days 48 and 51, was slightly higher in line R than in line R3.1, indicating that, at low irradiances, line R assimilated more carbon than line R3.1. Carboxylation efficiency (V_{max}) of yfd leaves on Days 50 and 51 (Table 1) was slightly higher in line R3.1 than in line R, paralleling the greater total Rubisco activity in this line.

The amount and total activity of Rubisco as well as chlorophyll concentration of life span leaves of line R (Figures 4A, 4B and 4D) were low in the young leaves, at their highest on the second sampling on Day 34, and decreased toward the end of the experiment. In yfd leaves of line R, the amount and total activity of Rubisco and the concentration of chlorophyll (Figures 4A, 4B and 4D) were highest on the first day of sampling, thereafter these parameters decreased steadily. In line R3.1, the amount and total activity of Rubisco and chlorophyll concentration (Figures 4A, 4B and 4D) remained stable throughout the study in both leaf types. The chlorophyll a/b ratio decreased from 4.0 to 3.3 in life span leaves of line R when upper leaves shaded them, whereas the chl a/b ratio remained around 4.0 in line R3.1. In the life span leaves of line R, total soluble protein concentration was highest (about 50 mg g_{FM}^{-1}) at the beginning of the study, but decreased later, whereas in line R3.1, total soluble protein concentration remained high throughout the study (33–46 mg g_{FM}^{-1}) (Figure 4C).

Electron microscopy of yfd leaves on Days 69–70 showed that cells of line R leaves contained larger plastoglobuli than cells of line R3.1 leaves (cf. Figures 5A and 5B). There were no ultrastructural abnormalities of the leaf cells of line R3.1. The chloroplasts in the palisade parenchyma cells were significantly ($P < 0.05$) larger in line R3.1 than in line R, but the starch grains and mitochondria were the same size in both lines (Table 2). In spongy mesophyll cells, the sizes of the chloroplasts, starch grains or mitochondria did not differ between the two lines.

Table 1. Photosynthetic rates (± SE) in the youngest fully developed leaves of silver birch lines R ($n = 20$) and R3.1 ($n = 6$) on Day 49. Net photosynthesis was measured at 360 ppm CO_2 and 40% relative humidity (RH) at saturating photosynthetically active radiation (PAR) > 800 μmol m^{-2} s^{-1}. Apparent quantum yield was measured from the initial slope of the light response curve PAR < 180 μmol m^{-2} s^{-1} at 360 ppm CO_2 and 40–55% RH. Maximum velocity of carboxylation was measured as the initial slope of the CO_2 response curve between 40 and 170 ppm CO_2. Abbreviations: P_n = net photosynthesis; g_s = stomatal conductance; C_i = intercellular CO_2 concentration; C_i/C_a = intercellular CO_2/atmospheric CO_2; VPD_{leaf} = leaf-to-air vapor pressure deficit; E = transpiration; α = apparent quantum yield; and V_{max} = maximum velocity of carboxylation.

Parameters	Line R	Line R3.1
P_n (μmol m^{-2} s^{-1})	9.2 ± 0.4	9.9 ± 1.2
g_s (mol H_2O m^{-2} s^{-1})	0.2 ± 0.0	0.2 ± 0.1
C_i (μmol mol^{-1})	219.7 ± 9.9	222.6 ± 16.3
E (mol H_2O m^{-2} s^{-1})	2.5 ± 0.3	2.5 ± 0.
VPD_{leaf} (kPa)	1.6 ± 0.0	1.6 ± 0.0
C_i/C_a	0.6 ± 0.0	0.7 ± 0.1
α	0.034	0.032
	$r^2 = 0.826$	$r^2 = 0.852$
V_{max}	0.0299	0.0314
	$r^2 = 0.955$	$r^2 = 0.866$

Changes in gene expression during leaf development

To select comparable leaf samples for reverse northern hybridization analysis (Table 3), the level of *RbcS1* mRNA (Figure 6A) and the amount and activity of Rubisco (Figures 4A and 4B) were assayed as indicators of different developmental stages during leaf ontogeny. The yfd leaf from Day 23 was chosen as the active photosynthesizing leaf. The life span leaves from Days 44 and 56 were selected to present the early and advanced phases of senescence, respectively. The actin 2 gene of *Arabidopsis thaliana* (L.) Heynh. was used as a constitutive control among the different reverse Northern mem-

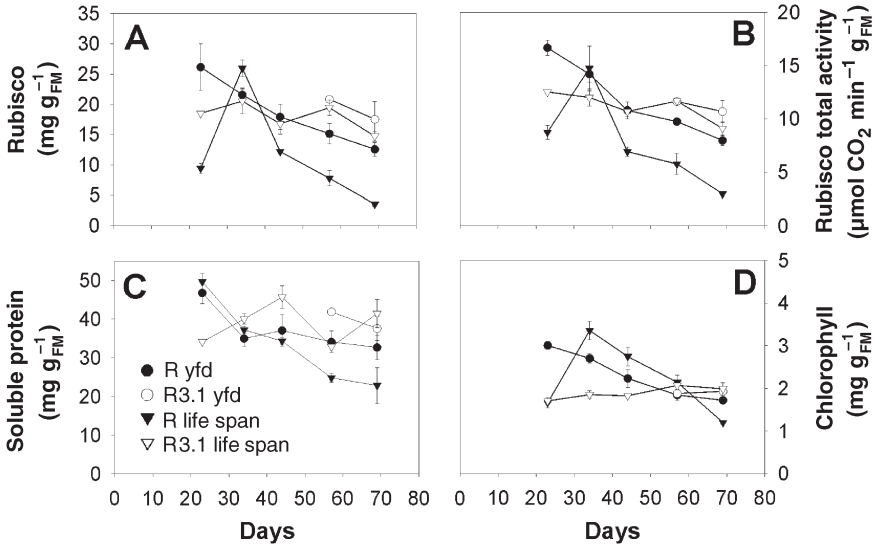

Figure 4. Amount of Rubisco (A), total activity of Rubisco (B), soluble protein concentration (C) and chlorophyll concentration (D) in the life span and youngest fully developed (yfd) leaves of silver birch lines R and R3.1 on Days 23, 34, 44, 57 and 69–70. Mean ± SE, n = 1–4.

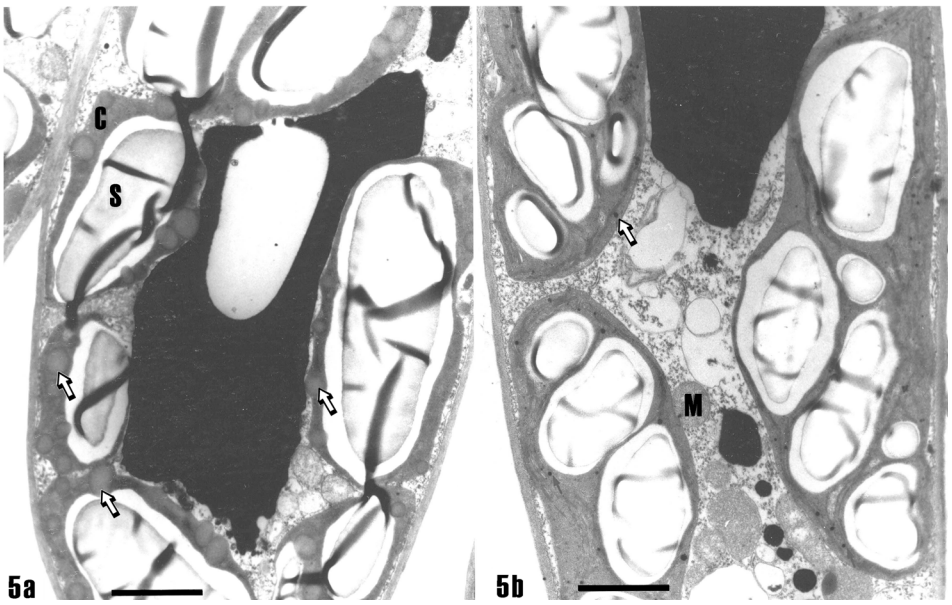

Figure 5. Parts of palisade cells from the youngest fully developed leaves of silver birch lines R and R3.1. In line R (5a), the mean area of each chloroplast (= C) was about 14 μm^2 and that of each starch grain (= S) was about 9 μm^2. Size of the plastoglobuli (arrows) varied greatly. In line R3.1 (5b), the mean area of each chloroplast was about 29 μm^2 and that of each starch grain was about 18 μm^2. Plastoglobuli were always electron dense and small. Abbreviation: M = mitochondria. Bars = 2 μm.

branes because its mRNA levels varied less than twofold in Northern hybridization analyses (data not shown) in the selected leaf samples.

Reverse Northern hybridization analysis showed differential expression of genes during leaf senescence (Table 1). The senescence-associated genes (SAGs) belonged to various functional subgroups including energy metabolism, cell maintenance and development, antioxidant and defence genes, hormone perception and phenylpropanoid biosynthesis. The expression of most of these genes increased as senescence advanced, but a decline in the expression of some genes was observed in senescing leaves compared with young leaves. In particular, photosynthesis-related genes, such as the small subunit of Rubisco (*RbcS1*), chlorophyll a/b binding protein (*Cab*) and carbonic anhydrase (*Ca*), as well as the genes of alpha-tubulin (*Atub*) and ACC synthase were down-regulated during leaf senescence (Table 3).

We used RNA dot blot hybridizations to confirm the results of the reverse Northern analyses, to reveal differences between lines R and R3.1, and to study changes in gene expression throughout the whole leaf life span. Six genes representing photosynthesis (*RbcS1* and *Cab*), cell maintenance (*Cyp1* and *Lox2*), antioxidants (*Apx*) and defence (*Pr1*) were chosen for the analyses. Two of these genes were down-regulated during senescence (*RbcS1*, *Cab*) and four of them were chosen (*Cyp1*, *Lox2*, *Apx*, *Pr1*) to represent SAGs.

The mRNA levels of *RbcS1* and *Cab* decreased during the experiment in the life span leaves of both lines (Figures 6A and 6B); however, the decreases occurred on different time scales in line R and line R3.1 (cf. Figures 6A and 6B). The *RbcS1* and *Cab* mRNA levels also decreased during the experiment in yfd leaves of line R but not of line R3.1. The expression of different SAGs varied temporally in the life span leaves of line R, so that *Cyp1* (Figure 6D) and *Pr1* (Figure 6F) were expressed at their maximum intensity on the last sampling day (Days 69–70), whereas expression of *Apx* and *Lox2* (Figures 6C and 6E) was highest on Day 56 and was decreasing on the last sampling day. In yfd leaves of line R, levels of *Apx* and *Lox2* increased toward the end of the experiment, whereas levels of *Cyp1* (Figure 6D) and especially *Pr1* (Figure 6F) were low. In both yfd and life span leaves of line R3.1, *Cyp1* (Figure 6D) and *Pr1* (Figure 6F) were at about the same low level as the basal expression in young leaves of line R. The level of *Lox2* mRNA increased more in line R3.1 than in line R on the last sampling day (Figure 6E).

Table 2. Mean organelle size (± SE) in the parenchyma palisade and spongy mesophyll cells of the youngest fully expanded leaves from silver birch lines R and R3.1 on Days 69–70. An asterisk denotes a statistically significant difference at $P < 0.05$.

	Line R	Line R3.1
Palisade parenchyma cells		
Chloroplasts	14.5 ± 3.2	28.6 ± 9.9 *
starch grains	9.2 ± 3.0	17.6 ± 11.6
Mitochondria	0.5 ± 0.1	0.4 ± 0.1
Spongy mesophyll cells		
Chloroplasts	12.0 ± 2.7	11.7 ± 0.8
starch grains	7.8 ± 2.4	4.0 ± 1.8
Mitochondria	0.4 ± 0.0	0.5 ± 0.1

Discussion

Senescence-related decline in photosynthesis is characterized by loss of chlorophyll (Gepstein 1988) and decreases in the amount and activity of Rubisco (Batt and Woolhouse 1975, Kasemir et al. 1988). A declining efficiency of light reactions, usually in the capacity of PSII, has been observed in senescing leaves (Gepstein 1988, Humbeck et al. 1996, Lu and Zhang

Table 3. Changes in gene expression during leaf development in silver birch normalized relative to the abundance of actin 2. Two stages of leaf senescence, represented by the life span leaves of Days 44 and 56, are compared with the active photosynthetic phase, represented by the youngest fully developed leaf (yfd) on Day 23. Relative transcript abundances are denoted by –/+ when the decrease/increase was two- to fivefold, – –/++ when the change was 5- to 10-fold, and – – –/+++ when the change was more than 10-fold. Under the heading "comments," "ws" indicates a weak signal in some leaf sample, "no" indicates that no difference was detected in the mRNA level. An asterisk indicates that the EST-sequences will appear in the Genbank as part of a larger group.

	Relative transcript abundance		
	Day 44 versus yfd	Day 56 versus yfd	Comments
Photosynthesis			
RbcS, small subunit of Rubisco, Y07779	– –	– – –	
Cab, chlorophyll a/b binding protein, est*	– –	– – –	
Ca, carbonic anhydrase, est*	– – –	– – –	
Energy production			
G6PD, glucose-6-phosphate dehydrogenase, AJ279688		+	
Mpt, mitochondrial phosphate translocator, Y08499	+	+	ws
Adh, alcohol dehydrogenase, AJ279698	++	++	ws
Cell maintenance and development			
Lox1, lipoxygenase 1, AY124318	++	+++	ws
Lox2, lipoxygenase 2, AY124319	+	+++	
Lap, leucine aminopeptidase, Y14777	+	+	
Cyp1, cysteine proteinase 1, AJ415385		+++	
Cyp2, cysteine proteinase 2, AJ415386	+	++	
Atub, alpha-tubulin, AJ279695	– –	– –	
Dad, defender against apoptotic cell death, AJ279687	+	+	
Dhn, dehydrin	+	+	
Antioxidants			
Apx, ascorbate peroxidase, AJ279686	+	++	
Gpx, glutathione peroxidase, AJ279689		++	
Gr, glutathione reductase, AJ279690	+	+	
Gst, glutathione-*S*-transferase, tau	+	+++	
Gst, glutathione-*S*-transferase, theta, AJ279691	++	+++	
Cu/Zn sod, Cu, Zn superoxide dismutase, AJ279694		+	
Cat, catalase, AJ295295			no
Defence genes			
Pr1, pathogenesis-related protein 1, AJ279696	++	+++	ws
Pr3a, acidic endochitinase, AJ279692	+	+++	
Ypr10, pathogenesis-related protein 10, X77601	+++	+++	
Wrky, DNA binding protein wrky, AJ279697	+	+++	ws
Hormone biosynthesis and perception			
Bp-Etr, ethylene receptor	++	+	ws
Bp-Aco1, ACC oxidase, Y10749			no
Bp-Acs1, ACC synthase, AY120897	– –	–	ws
Aos, allene oxide synthase, est*			no
Phenylpropanoid biosynthesis			
DS3, 3-deoxy-D-arabinoheptulosonate-7-phosphate synthase		+	
Pal, phenylalanine ammonium lyase, X76077	++	+++	
Chs, chalcone synthase, Y11022	++	++	

1998). On the molecular level, the expression of photosynthesis-specific genes decreases as leaf senescence advances (Bate et al. 1991, Jiang et al. 1993). We observed declines in photosynthesis, in the amount and activity of Rubisco, in chlorophyll concentration and in the level of *RbcS1* mRNA in life span leaves of line R soon after they were fully expanded. A similar decline in photosynthesis starting as soon as the leaves are fully expanded has been reported in birch (Valjakka et al. 1999) and *Arabidopsis* (Stessman et al. 2002, Buchanan-Wollaston et al. 2003).

Photosynthetic activity of the youngest fully developed leaves was maintained throughout the experimental period, indicating that the youngest leaves remain active and that the accumulation of biomass continues after height growth cessation. However, at the time of height growth cessation in line R, the yfd leaves were smaller and steady decreases in the amount

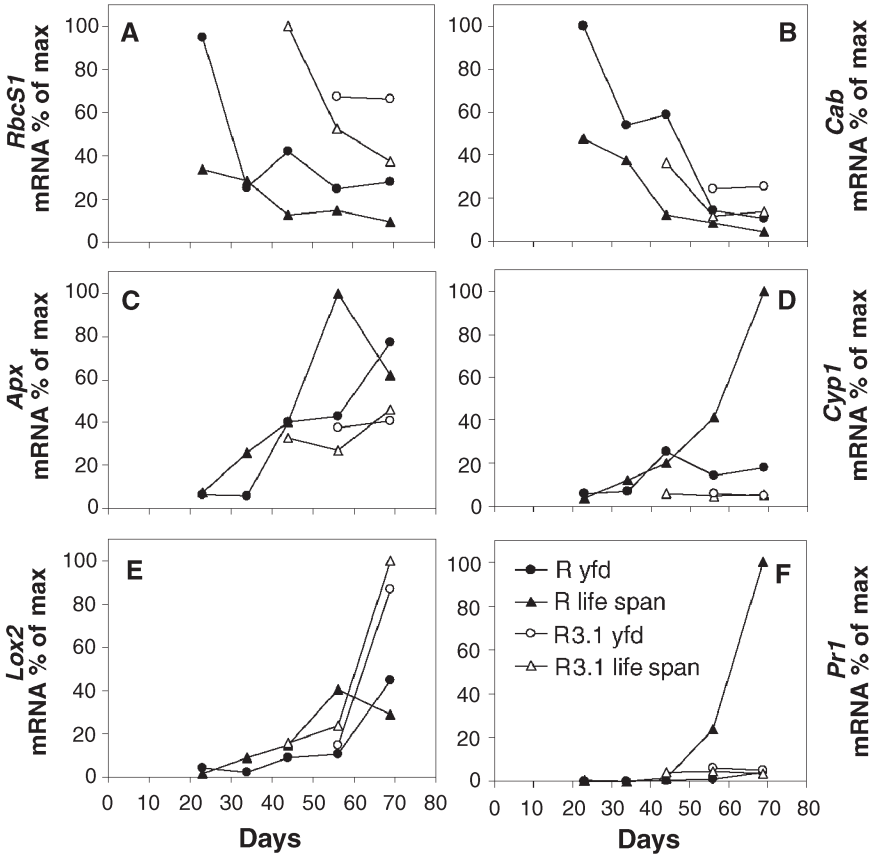

Figure 6. Relative mRNA levels of the small subunit of Rubisco (*RbcS1*) (A), chlorophyll a/b binding protein (*Cab*) (B), ascorbate peroxidase (*Apx*) (C), cysteine proteinase (*Cyp1*) (D), lipoxygenase (*Lox2*) (E) and pathogenesis-related protein 1 (*Pr1*) (F) on Days 23, 34, 44, 57 and 69–70, based on RNA-dot blot hybridization analysis. The mRNA levels were normalized based on 18S rRNA levels.

and total activity of Rubisco and chlorophyll concentration were observed (cf. Valjakka et al. 1999).

Delayed leaf senescence in line R3.1 was manifest in several ways. In life span leaves that had developed at the same time, the onset and rate of decline in photosynthesis differed markedly between lines R and R3.1. The life span leaves of R3.1 resembled the yfd leaves of line R more closely than the corresponding line R life span leaves. Compared with line R leaves, line R3.1 leaves displayed a delayed decline in all of the photosynthetic parameters measured. Compared with those of line R3.1, yfd leaves of line R had larger plastoglobuli and smaller chloroplasts in the palisade parenchyma cells, characteristics that may be interpreted as signs of senescence (Dodge 1970, Inada et al. 1998, Guiamét et al. 1999). Although the mRNA levels of *RbcS1* were generally higher in line R3.1 than in line R, we found no evidence of overproduction of *RbcS1* in line R3.1 compared with line R. Thus, the phenotype of line R3.1 can be considered the result of insertional mutagenesis.

Life span leaves of line R became self-shaded by new leaves that developed above them. Low irradiances may have accelerated senescence in the line R life span leaves, as has been observed in *Helianthus annuus* L. (Rousseaux et al. 1996), and as a result of vigorous growth, the life span leaves of line R may have become source leaves for nitrogen (Masclaux et al. 2000). In contrast, the life span leaves of R3.1 received less light than the R leaves because of the smaller height of the line R3.1 plants and their random positioning among the taller line R plants. Therefore, the delayed leaf senescence of line R3.1 cannot be explained by better light conditions. Another possibility is that, as a consequence of the slow growth of line R3.1, reallocation of nutrients may not have occurred when the measurements were made. We cannot, therefore, rule out the possibility that the delay in leaf senescence in line R3.1 is related to its overall low growth rate or is associated with different nutrient conditions compared with line R.

Only a limited EST library is available for the *Betula* family to study gene expression during the different phases of active leaf growth and leaf senescence. We found changes in the expression of 32 genes, belonging to different functional classes, during leaf senescence. The genes down-regulated during senescence were mostly photosynthesis-related (*RbcS*, *Cab*, *Ca*) or associated with cell maintenance (*Atub*). Decreased abundance of *RbcS* and *Cab* transcripts has previously been reported during leaf senescence in bean and soybean (Bate et al. 1991, Jiang et al. 1993). We observed decreased expression of the *RbcS1* gene in both yfd and life span leaves of line R during the experiment, and in the life span leaves of line R3.1. Throughout our study, the *Cab* gene was expressed at a relatively low level in line R3.1 compared with line R. In contrast, genes associated with energy metabolism, *G6PD*, *Adh* and *Mpt,* had higher transcript levels in senescing leaves than in growing leaves, indicating changes in energy production. Similarly, genes related to respiration and mitochondrial energy

conversion are reported to be upregulated in autumn leaves of aspen (Bhalerao et al. 2003, Andersson et al. 2004).

Nitrogen mobilization from senescing leaves involves proteases. Some senescence-associated cysteine proteases have a basal expression level in young leaves (Drake et al. 1996, Xu and Chye 1999, Ueda et al. 2000), whereas others are highly specific for senescence (Noh and Amasino 1999). In aspen, expression of eight cysteine proteases increases as senescence proceeds, and their respective patterns differ (Andersson et al. 2004). Cysteine proteases are the most abundantly expressed gene family during senescence of *Arabidopsis* leaves (Guo et al. 2004). The *Cyp1* mRNA level in line R3.1 remained low, whereas it increased in line R simultaneously with the decline in photosynthesis and the onset of leaf senescence, indicating that *Cyp1* could serve as a molecular marker of senescence in silver birch.

Several genes associated with cell maintenance and development were upregulated as leaf senescence advanced. For example, increased expression of *Lap* mRNA, previously observed in senescing birch leaves by Valjakka et al. (1999), indicates increased protein degradation during leaf senescence. The level of *Lox2* mRNA decreased during the advanced stage of senescence in life span leaves of line R, whereas *Lox2* expression was high in both the yfd and life span leaves of line R3.1 at the end of the experiment. Products of LOX metabolism play important roles in development and in responses to stress (Porta and Rocha-Sosa 2002). Stress-inducible genes may help to maintain cell viability during the early stages of senescence. Alternatively, the observed induction of lipoxygenases, coded for by the *Lox1* and *Lox2* genes, after the decline in photosynthesis in the life span leaves of line R could be related to increasing breakdown of membranes, because lipoxygenases are involved in membrane degradation (Thompson et al. 1998).

We found increased expression of *Dhn* in the leaves during both early and advanced stages of senescence, which has not previously been studied during leaf senescence. However, increased expression of dehydrin-like proteins has been reported in the senescing leaves of *Arabidopsis* (Buchanan-Wollaston et al. 2003) and aspen (Bhalerao et al. 2003).

Production of reactive oxygen species (ROS) is enhanced during leaf senescence (Thompson et al. 1987) and this is accompanied by the production of certain antioxidant enzymes (Buchanan-Wollaston 1997). The antioxidative capacity of senescing leaves may change at different rates in different organelles. During natural senescence of cucumber (*Cucumis sativus* L.) leaves, the activities of ascorbate peroxidase (APX) and glutathione peroxidase (GPX) increased, whereas the activities of glutathione reductase (GR), superoxide dismutase (SOD) and catalase (CAT) decreased (Kanawaza et al. 2000). In detached spinach (*Spinachia oleracea* L.) leaves, the activities of APX, CAT, GR and SOD decreased (Hodges and Forney 2000). In isolated peroxisomes and mitochondria from pea (*Pisum sativum* L.), APX activity decreased in both organelles, GR activity decreased in the mitochondria but not in the peroxisomes, and Mn-SOD activity decreased in the mitochondria (Jiménez et al. 1998). In our study, mRNA levels of *Apx*, *Gpx*, *GR*, *Gst* and *Cu*, *Zn-SOD* increased during leaf senescence. Detailed analysis indicated that *Apx* transcript levels in line R increased in aging life span leaves, but decreased during the advanced stages of senescence. The timing of *Apx* expression during the life of a leaf suggests that APX is involved in H_2O_2 detoxification before leaf senescence, and that the capacity for H_2O_2 scavenging gradually declines as senescence proceeds (Hodges and Fourney 2000).

Many pathogenesis-related PR protein genes are induced during senescence, including the genes coding for PR-1a-like protein of *Brassica napus* L. (Hanfrey et al. 1996) and several chitinases of parsley (*Petroselinum crispum* (Mill.) Nyman ex A. W. Hill) (Lers et al. 1998), as well as *PR1* of aspen (Bhalerao et al. 2003), *Ypr10* of soybean (*Glycine max*) (Crowell et al. 1992) and *Ypr10* of silver birch (Valjakka et al. 1999). The transcript levels of the PR-proteins 1, 3a, and 10 increased in leaves of line R as the leaves aged, but were low in leaves of line R3.1. Several signaling pathways involved in the induction of PR-protein genes, such as sugars (Hebers et al. 1996), ethylene (Eyal et al. 1992), ROS (Surplus et al. 1998) and salicylic acid (Yalpani et al. 1991) can regulate leaf senescence; however, the exact role of PR proteins in senescing leaves is unknown. These proteins may establish a stage of increased protection against potentially invasive pathogens during the phase when soluble sugars and amino acids are transported from the leaves. The PR protein genes may also respond to the signals, such as ROS, ethylene or SA that are involved in the regulation of senescence. Among other defence genes, *Wrky*, a transcription factor that has been associated with both senescence and defence (Robatzek and Somssich 2001), was highly induced during leaf senescence.

Phenolic compounds often accumulate in response to various stresses and during senescence, and there is increasing evidence that several products of the phenylpropanoid pathway are involved in protection from oxidative stress (Yamasaki 1997, Yamasaki et al. 1997, Tamagnone et al. 1998, Hoch et al. 2001). In our study, based on the increasing mRNA levels of DAHP-synthase (*DS3*) and *Pal*, the biosynthetic pathway of phenolic compounds was active during birch leaf senescence. Up-regulation of several enzymes of the phenylpropanoid pathway may be necessary to produce flavonoids that serve as electron donors and are readily oxidized by peroxidases during H_2O_2 detoxification (Yamasaki et al. 1997).

In conclusion, we found that the transgenic line R3.1 showed delayed age-dependent leaf senescence compared with the wild-type line R. The age-dependent senescence of the lower leaves on the stem was characterized by declines in photosynthesis, amount and activity of Rubisco, chlorophyll concentration and in the levels of *RbcS1* and *Cab* mRNA. After photosynthesis declined, the transcript levels of many senescence-associated genes became more abundant. A detailed analysis of transcript abundances during leaf development showed that, during the advanced stage of senescence, *Cyp1* and *Pr1* mRNA levels increased, whereas the expression of *Apx* and *Lox2* decreased. Thus *Apx* and *Lox2* might function in enhanced housekeeping activities rather than playing a highly senescence-specific role. To increase our understanding of se-

nescence, further information is needed concerning changes in gene expression, enzyme activities and interaction of environmental and metabolic signals during the life span of a leaf. For this work, the late-senescing R3.1 line might be a useful tool.

Acknowledgements

We thank Mr. Jouko Lehto, Ms. Aila Viinanen, Ms. Taina Naukkarinen, Ms. Marja-Leena Jalkanen and Ms. Mervi Ahonpää for skillful technical assistance during this experiment, and Dr. Joann von Weissenberg for revising the English language. The research groups of Prof. E.T. Palva and Prof. J. Kangasjärvi are thanked for the cDNA probes used. This study was funded by grants from the Finnish Ministry of Agriculture and Forestry (to EV), the Academy of Finland, Grant 44248 (to HH) and by the Finnish Centre of Excellence program (2000–2005, JK).

References

Andersson, A., J. Keskitalo, A. Sjödin et al. 2004. A transcriptional timetable of autumn senescence. Genome Biol. 5:R24.

Bate, N.J., S.J. Rothstein and J.E. Thompson. 1991. Expression of nuclear and chloroplast photosynthesis-specific genes during leaf senescence. J. Exp. Bot. 42:801–811.

Batt, T. and H.W. Woolhouse. 1975. Changing activities during senescence and sites of synthesis of photosynthetic enzymes in leaves of the Labiate, *Perilla frutescens* (L.) Britt. J. Exp. Bot. 26:569–579.

Bhalerao, R., J. Keskitalo, F. Sterky et al. 2003. Gene expression in autumn leaves. Plant Physiol. 131:430–442.

Bilger, W. and O. Björkman. 1990. Role of xanthophyll cycle in photoprotection elucidated by measurements of light-induced absorbance changes, fluorescence and photosynthesis in *Hedera canariensis*. Photosynth. Res. 25:173–185.

Bowler, C. and R. Fluhr. 2000. The role of calcium and activated oxygens as signals for controlling cross-tolerance. Trends Plant Sci. 5:241–246.

Bradford, M.M. 1976. A rapid and sensitive method for the quantitation of microgram quantities of protein utilizing the principle of protein-dye binding. Anal. Biochem. 72:248–254.

Brendley, B.W. and E.J. Pell. 1998. Ozone-induced changes in biosynthesis of Rubisco and associated compensation to stress in foliage of hybrid poplar. Tree Physiol. 18:81–90.

Buchanan-Wollaston, V. 1997. The molecular biology of leaf senescence. J. Exp. Bot. 48:181–199.

Buchanan-Wollaston, V., S. Earl, E. Harrison, E. Mathas, S. Navabpour, T. Page and D. Pink. 2003. The molecular analysis of leaf senescence—a genomics approach. Plant Biotech. J. 1:3–22.

Chang, S., J. Puryear and C. Cairney. 1993. A simple and efficient method for isolating RNA from pine trees. Plant Mol. Biol. Rep. 11:113–116.

Church, G.M. and W. Gilbert. 1984. Genomic sequencing. Proc. Natl. Acad. Sci. USA 81:1991–1995.

Crowell, D.N., M.E. John, D. Russell and R.M. Amasino. 1992. Characterization of a stress-induced, developmentally regulated gene family from soybean. Plant Mol. Biol. 18:459–466.

Dodge, J.D. 1970. Changes in chloroplast fine structure during the autumnal senescence of *Betula* leaves. Ann. Bot. 34:817–824.

Drake, R., I. John, A. Farrell, W. Cooper, W. Schuch and D. Grierson. 1996. Isolation and analysis of cDNAs encoding tomato cysteine proteases expressed during leaf senescence. Plant Mol. Biol. 30: 755–767.

Eyal, Y., O. Sagee and R. Fluhr. 1992. Dark-induced accumulation of a basic pathogenesis-related (PR-1) transcript and a light requirement for its induction by ethylene. Plant Mol. Biol. 19:589–599.

Gan, S. and R.M. Amasino. 1997. Making sense of senescence; molecular genetic regulation and manipulation of leaf senescence. Plant Physiol. 113:313–319.

Genty, B., J.-M. Briantais and N.R. Baker. 1989. The relationship between quantum yield of photosynthetic electron transport and quenching of chlorophyll fluorescence. Biochim. Biophys. Acta 990:87–92.

Gepstein, S. 1988. Photosynthesis. *In* Senescence and Aging in Plants. Eds. L.D. Noodén and A.C. Leopold. Academic Press, San Diego, CA, pp 85–109.

Gepstein, S. 2004. Leaf senescence—not just a "wear and tear" phenomenon. Genome Biol. 5:212.

Gepstein S., G. Sabehi, M.-J. Carp, T. Hajouj, M.F.O. Nesher, I.Y.C. Dor, M. Bassani. 2003. Large-scale identification of leaf senescence-associated genes. Plant J. 36:629–642.

Guiamét, J.J. and M.C. Giannibelli. 1994. Inhibition of the degradation of chloroplast membranes during senescence in nuclear 'stay green' mutants of soybean. Physiol. Plant. 91:395–402.

Guiamét, J.J., E. Pichersky and L.D. Noodén. 1999. Mass exodus from senescing soybean leaves. Plant Cell Physiol. 40:986–992.

Guo, Y., Z. Cai and S. Gan. 2004. Transcriptome of *Arabidopsis* leaf senescence. Plant Cell Environ. 27:521–549.

Hanfrey, C., M. Fife and V. Buchanan-Wollaston. 1996. Leaf senescence in *Brassica napus*: expression of genes encoding pathogenesis-related proteins. Plant Mol. Biol. 30:597–609.

Hebers, K., P. Meuwly, J.-P. Métraux and U. Sonnewald. 1996. Salicylic acid-independent induction of pathogenesis-related protein transcripts by sugars is dependent on leaf developmental stage. FEBS Lett. 397:239–244.

Hensel, L.L., V. Grbic, D.A. Baumgarten and A.B. Bleecker. 1993. Developmental and age-related processes that influence the longevity and senescence of photosynthetic tissues in *Arabidopsis*. Plant Cell 5:553–564.

Hoch, W.A., E.L. Zeldin and B.H. McCown. 2001. Physiological significance of anthocyanins during autumnal leaf senescence. Tree Physiol. 21:1–8.

Hodges, D.M. and C.F. Forney. 2000. The effects of ethylene, depressed oxygen and elevated carbon dioxide on antioxidant profiles of senescing spinach leaves. J. Exp. Bot. 51:645–655.

Humbeck, K., S. Quast and K. Krupinska. 1996. Functional and molecular changes in the photosynthetic apparatus during senescence of flag leaves from field-grown barley plants. Plant Cell Environ. 19:337–344.

Inada, N., A. Sakai, H. Kuroiwa and T. Kuroiwa. 1998. Three-dimensional analysis of the senescence program in rice (*Oryza sativa* L.) coleoptiles. Investigations of tissues and cells by fluorescence microscopy. Planta 205:153–164.

Jiang, C.-Z., S.R. Rodermel and R.M. Shibles. 1993. Photosynthesis, Rubisco activity and amount, and their regulation by transcription in senescing soybean leaves. Plant Physiol. 101:105–112.

Jiménez, A., J.A. Hernández, G. Pastori, L.A. del Río and F. Sevilla. 1998. Role of the ascorbate-glutathione cycle of mitochondria and peroxisomes in the senescence of pea leaves. Plant Physiol. 118: 1327–1335.

Jordi, W., A. Schapendonk, E. Davelaar, G.M. Stoopen C.S. Pot, R. de Visser, J.A. van Rhijn, S. Gan and R.M. Amasino. 2000. Increased cytokinin levels in transgenic P_{SAG12}-*IPT* tobacco plants have large direct and indirect effects on leaf senescence, photosynthesis and N partitioning. Plant Cell Environ. 23:279–289.

Kanawaza, S., S. Sano, T. Koshiba and T. Ushimaru. 2000. Changes in antioxidative enzymes in cucumber cotyledons during natural senescence: comparison with those during dark-induced senescence. Physiol. Plant. 109:211–216.

Kasemir, H., D. Rosemann and R. Oelmüller. 1988. Changes in ribulose-1,5-bisphosphate carboxylase and its translatable small subunit mRNA levels during senescence of mustard (*Sinapis alba*) cotyledons. Physiol. Plant. 73:257–264.

Laitinen, K., E.-M. Luomala, S. Kellomäki and E. Vapaavuori. 2000. Carbon assimilation and nitrogen in needles of fertilized and unfertilized field-grown Scots pine at natural and elevated concentrations of CO_2. Tree Physiol. 20:881–892.

Lers, A., W.B. Jiang, E. Lomaniec and N. Aharoni. 1998. Proteins functionally and immunogenically related to pathogenesis-related proteins are induced during parsley leaf senescence. Physiol. Plant. 103:497–502.

Lu, C. and J. Zhang. 1998. Changes in photosystem II function during senescence of wheat leaves. Physiol. Plant. 104:239–247.

Masclaux, C., M.-H. Valadier, N. Brugière, J.-F. Morot-Gaudry and B. Hirel. 2000. Characterization of the sink/source transition in tobacco (*Nicotiana tabacum* L.) shoots in relation to nitrogen management and leaf senescence. Planta 211:510–518.

Miller, A., C. Schlagnhaufer, M. Spalding and S. Rodermel. 2000. Carbohydrate regulation of leaf development: prolongation of leaf senescence in Rubisco antisense mutants of tobacco. Photosynth. Res. 63:1–8.

Noh, Y.-S. and R.M. Amasino. 1999. Regulation of developmental senescence is conserved between *Arabidopsis* and *Brassica napus*. Plant Mol. Biol. 41:195–206.

Ori, N., M.T. Juarez, D. Jackson, J. Yanaguchi, G.M. Banowetz and S. Hake. 1999. Leaf senescence is delayed in tobacco plants expressing the maize homeobox *knotted1* under the control of a senescence-activated promoter. Plant Cell 11:1073–1080.

Pell, E.J., J.P. Sinn, B.W. Brendley, L. Samuelson, C. Vinten-Johansen, M. Tien and J. Skillman. 1999. Differential response of four tree species to ozone-induced acceleration of foliar senescence. Plant Cell Environ. 22:779–790.

Porra, R.J., W.A. Thompson and P.E. Kriedemann. 1989. Determination of accurate extinction coefficients and simultaneous equations for assaying chlorophylls a and b extracted with four different solvents: verification of the concentration of chlorophyll standards by atomic absorption spectroscopy. Biochim. Biophys. Acta 975: 384–394.

Porta, H. and M. Rocha-Sosa. 2002. Plant lipoxygenases. Physiological and molecular features. Plant Physiol. 130:15–21.

Robatzek, S. and I.E. Somssich. 2001. A new member of the *Arabidopsis* WRKY transcription factor family, *At*WRKY6, is associated with both senescence- and defence-related processes. Plant J. 28:123–133.

Romppanen, T. and Y. Collan. 1984. Practical guidelines for a morphometric study. *In* Stereology and Morphometry in Pathology. Eds. Y. Collan, M.-L. Aalto, V.-M. Kosma, A. Naukkarinen, T. Romppanen and K. Syrjänen. Kuopio University Press, Kuopio, Finland, pp 72–95.

Rousseaux, M.C., A.J. Hall and R.A. Sánches. 1996. Far-red enrichment and photosynthetically active radiation level influence leaf senescence in field-grown sunflower. Physiol. Plant. 96:217–224.

Ruuska, S.A., E.M. Vapaavuori and A. Laisk. 1994. Reactions of birch leaves to changes in light during early ontogeny: comparison between in vivo and in vitro techniques to measure carbon uptake. J. Exp. Bot. 45:343–353.

Sambrook, J., T. Maniatis and E.F. Fritsch. 1989. Molecular cloning. 2nd Edn. Cold Spring Harbor Laboratory Press, Cold Spring Harbor, NY, 1659 p.

Smart, C.M. 1994. Gene expression during leaf senescence. New Phytol. 126:419–488.

Soikkeli, S. 1980. Ultrastructure of the mesophyll in Scots pine and Norway spruce: seasonal variation and molarity of the fixative buffer. Protoplasma 103:241–252.

Stessman, D.A. Miller, M. Spalding and S. Rodermel. 2002. Regulation of photosynthesis during *Arabidopsis* leaf development in continuous light. Photosynth. Res. 72:27–37.

Surplus, S.L., B.R. Jordan, A.M. Murphy, J.P. Carr, B. Thomas and S.A.-H. Mackerness. 1998. Ultraviolet-B-induced responses in *Arabidopsis thaliana*: role of salicylic acid and reactive oxygen species in the regulation of transcripts encoding photosynthetic and acidic pathogenesis-related proteins. Plant Cell Environ. 21: 685–694.

Tamagnone, L., A. Merida, N. Stacey et al. 1998. Inhibition of phenolic acid metabolism results in precocious cell death and altered cell morphology in leaves of transgenic tobacco plants. Plant Cell 10: 1801–1816.

Thomas, H. and C.M. Smart. 1993. Crops that stay green. Ann. Appl. Biol. 123:193–219.

Thompson, J.E., R.L. Legge and R.F. Barber. 1987. The role of free radicals in senescence and wounding. New Phytol. 105:317–344.

Thompson, J.E., C.D. Froese, E. Madey, M.D. Smith and Y. Hong. 1998. Lipid metabolism during plant senescence. Prog. Lipid Res. 37:119–141.

Ueda, T., S. Seo, Y. Ohashi and J. Hashimoto. 2000. Circadian and senescence-enhanced expression of tobacco cysteine protease gene. Plant Mol. Biol. 44:649–657.

Valjakka, M., E. Tuhkanen, J. Kangasjärvi and E. Vapaavuori. 1999. Expression of photosynthesis and senescence-related genes during leaf development and senescence in silver birch (*Betula pendula* Roth) seedlings. Physiol. Plant. 106:302–310.

Valjakka, M., T. Aronen, J. Kangasjärvi, E. Vapaavuori and H. Häggman. 2000. Genetic transformation of silver birch (*Betula pendula* Roth) by particle bombardment. Tree Physiol. 20:607–613.

Vapaavuori, E.M. and A.H. Vuorinen. 1989. Seasonal variation in the photosynthetic capacity of a willow (*Salix* cv. *Aquatica gigantea*) canopy. 1. Changes in the activity and amount of ribulose 1,5-bisphosphate carboxylase-oxygenase and the content of nitrogen and chlorophyll at different levels in the canopy. Tree Physiol. 5: 423–444.

Vicentini, F., S. Hörtensteiner, M. Schellenberg, H. Thomas and P. Matile. 1995. Chlorophyll breakdown in senescent leaves: identification of the biochemical lesion in a stay-green genotype of *Festuca pratensis* Huds. New Phytol. 129:247–252.

von Caemmerer, S. and G.D. Farquhar. 1981. Some relationships between the biochemistry of photosynthesis and the gas exchange of leaves. Planta 153:376–387.

Xu, F.-X. and M.-L. Chye. 1999. Expression of cysteine proteinase during developmental events associated with programmed cell death in brinjal. Plant J. 17:321–327.

Yalpani, N., P. Silverman, T.M.A. Wilson, D.A. Kleier and I. Raskin. 1991. Salicylic acid is a systemic signal and an inducer of pathogenesis-related proteins in virus-infected tobacco. Plant Cell 3: 809–818.

Yamasaki, H. 1997. A function of colour. Trends Plant Sci. 2:7–8.

Yamasaki, H., Y. Sakihama and N. Ikehara. 1997. Flavonoid-peroxidase reaction as a detoxification mechanism of plant cells against H_2O_2. Plant Physiol. 115:1405–1412.